J. Nonlinear Sci. Vol. 2: pp. 241–262 (1992)

Journal of Nonlinear Science

Multiple Lie–Poisson Structures, Reductions, and Geometric Phases for the Maxwell–Bloch Travelling Wave Equations

D. David[1] and D. D. Holm[2]

[1] Mathematics Department, Southern Methodist University, Dallas, TX 75275, USA
[2] Theoretical Division and Center for Nonlinear Studies, Los Alamos National Laboratory, Los Alamos, NM 87545, USA

Received May 10, 1990; accepted for publication
Communicated by Jerrold Marsden

Summary. The real-valued Maxwell-Bloch equations on $\mathbb{R}^3$ are investigated as a Hamiltonian dynamical system obtained by applying an S^1 reduction to an invariant subsystem of a dynamical system on $\mathbb{C}^3$. These equations on $\mathbb{R}^3$ are bi-Hamiltonian and possess several inequivalent Lie-Poisson structures parametrized by classes of orbits in the group $SL(2, \mathbb{R})$. Each Lie-Poisson structure possesses an associated Casimir function. When reduced to level sets of these functions, the motion takes various symplectic forms, from that of the pendulum to that of the Duffing oscillator. The values of the geometric (Hannay-Berry) phases obtained in reconstructing the solutions are found to depend upon the choice of Casimir function, that is, upon the parametrization of the reduced symplectic space.

1. Introduction

In self-induced transparency, radiation energy leaves the leading edge of an optical laser pulse, coherently excites the atoms of a resonant dielectric medium, and then returns to the trailing edge of the pulse with no loss, but with a delay caused by temporary storage of pulse energy in the atoms. The physics of self-induced transparency is reviewed in Allen and Eberly [1987]. To the extent that resonant interaction of coherent light with a medium calls into play only a single atomic transition and the laser may be taken to be monochromatic, the medium has effectively only two levels. For sufficiently short pulse duration, the coherent interaction between the pulse and the medium leading to self-induced transparency may be taken to be lossless. For most lasers and most atoms, this two-level lossless model is an excellent

approximation and is quite adequate for an understanding of the basic physics behind many coherent transient phenomena. Self-induced transparency equations based upon this model are derived from the Maxwell-Schrödinger equations in Holm and Kovacic [1991] by averaging over fast phases in the variational principle for the Maxwell-Schrödinger equations. A sketch of that derivation is given now in order to facilitate the considerations of the rest of the paper.

The dimensionless Maxwell-Schrödinger equations (Holm and Kovacic [1991]) are

$$\begin{aligned} E_{zz} - E_{tt} &= 2\kappa P_{tt}, \\ \dot{a}_+ &= \frac{1}{2\kappa} a_+ - E a_-, \\ \dot{a}_- &= \frac{1}{2\kappa} a_- - E a_+, \end{aligned} \tag{1.1}$$

where E denotes the electric field, P is the polarizability written in terms of two atomic-level amplitudes a_+ and a_- as $P = (a_+ a_-^* + a_+^* a_-)$, and the ratio of frequencies, $\kappa = \omega_c/\omega_0 \ll 1$, is a small parameter. Here ω_0 is the atomic transition frequency, and $\omega_c = (2\pi n d^2 \omega_0/\hbar)^{1/2}$ is the cooperative frequency of the medium with dipole density n and atomic dipole moment d. The wave equation for the linearly polarized electric field E follows from Maxwell's equations

$$\dot{D} = B_z, \qquad \dot{B} = E_z, \tag{1.2}$$

where $D = E + 2\kappa P$ is the electric displacement and B is the magnetic field.

Introducing the magnetic vector potential A that satisfies the relations $\dot{A} = E$ and $A_z = B$ allows us to write the primitive Maxwell-Schrödinger equations as stationarity conditions for Hamilton's principle, $\delta S = 0$, with action S given by

$$\begin{aligned} S = \int \Big[&\frac{1}{2}\dot{A}^2 - \frac{1}{2}A_z^2 + 2\kappa \dot{A}(a_+ a_-^* + a_+^* a_-) - (|a_+|^2 - |a_-|^2) \\ &+ i\kappa(a_+^* \dot{a}_+ - a_+ \dot{a}_+^* + a_-^* \dot{a}_- - a_- \dot{a}_-^*) \Big] \, dz \, dt. \end{aligned} \tag{1.3}$$

The third term in the integrand of S is the interaction term, which couples the electromagnetic field to the matter fields. Stationary variations with respect to A, a_+^*, and a_-^* give

$$\begin{aligned} \delta A: &\qquad \ddot{A} + 2\kappa \dot{P} - A_{zz} = 0, \\ \delta a_+^*: &\qquad i\dot{a}_+ - \frac{1}{2\kappa} a_+ + E a_- = 0, \\ \delta a_-^*: &\qquad i\dot{a}_- + \frac{1}{2\kappa} a_- + E a_+ = 0. \end{aligned} \tag{1.4}$$

Next, we write the atomic amplitudes in "rotating wave" form,

$$a_+ = u e^{-i(t-z)/2\kappa}, \qquad a_- = v e^{+i(t-z)/2\kappa}. \tag{1.5}$$

We also take the self-consistent part of the vector potential to be a modulated right-going wave, in the envelope form,

$$A = i\kappa w e^{-i(t-z)/\kappa} - i\kappa w^* e^{i(t-z)/\kappa}, \tag{1.6}$$

with the complex envelope function w. In these expressions, the complex envelope functions u,v, and w are assumed to depend only on time, t. Now the electric field is given by

$$E = \dot{A} = w e^{-i(t-z)/\kappa} + w^* e^{i(t-z)/\kappa} + O(\kappa). \tag{1.7}$$

So, to first order in κ, the quantity w is the complex electric field envelope. Now, averaging the action S over the fast phases, performing the z-integration, dividing by 4κ, and dropping terms of higher order in κ yields the new action

$$\bar{S} = \int \left[i(w^*\dot{w} - w\dot{w}^*) + i(u^*\dot{u} - u\dot{u}^*) + i(v^*\dot{v} - v\dot{v}^*) + wu^*v + w^*uv^* \right] dt. \tag{1.8}$$

Varying the averaged action $\bar{S}$ yields

$$\begin{aligned} \delta\bar{S} = \int \{ & \delta w^* \left[i\dot{w} + uv^* \right] + \delta w \left[-i\dot{w}^* + u^*v \right] \\ & + \delta u^* \left[i\dot{u} + vw \right] + \delta u \left[-i\dot{u}^* + v^*w^* \right] \\ & + \delta v^* \left[i\dot{v} + uw^* \right] + \delta v \left[-i\dot{v}^* + u^*w \right] \} \, dt. \end{aligned} \tag{1.9}$$

Thus, stationarity of the averaged action $\bar{S}$ implies the Maxwell-Schrödinger envelope equations

$$\dot{w} = iuv^*, \quad \dot{u} = ivw, \quad \dot{v} = iuw^*. \tag{1.10}$$

Holm and Kovacic [1991] point out that these envelope equations are Hamiltonian on $\mathbb{C}^3$ with Hamiltonian function

$$H(u, v, w) = -\frac{1}{2}(u^*vw + uv^*w^*), \tag{1.11}$$

and symplectic form, $-1/2i\left[dw \wedge dw^* + du \wedge du^* + dv \wedge dv^*\right]$. In addition to H, these equations possess two extra constants of motion,

$$C = |u|^2 + |v|^2 \quad \text{and} \quad C' = |w|^2 + |u|^2, \tag{1.12}$$

since H is invariant under the two S^1 transformations

$$u \to e^{i\theta}u, \quad v \to e^{i\theta}v, \quad \text{and} \quad w \to e^{i\varphi}w, \quad u \to e^{i\varphi}u, \tag{1.13}$$

generated by C and C', respectively. The Hamiltonian vector field is given by

$$X_H = 2i\left(\frac{\partial H}{\partial u}\frac{\partial}{\partial u^*} - \frac{\partial H}{\partial u^*}\frac{\partial}{\partial u}\right) + 2i\left(\frac{\partial H}{\partial v}\frac{\partial}{\partial v^*} - \frac{\partial H}{\partial v^*}\frac{\partial}{\partial v}\right) + 2i\left(\frac{\partial H}{\partial w}\frac{\partial}{\partial w^*} - \frac{\partial H}{\partial w^*}\frac{\partial}{\partial w}\right). \tag{1.14}$$

The five-dimensional Maxwell-Bloch system (see, e.g., Puccioni et al. [1987]) is obtained by reducing the system (1.10) on $\mathbb{C}^3$ through the S^1 group action in θ generated by the constant C. We introduce the following transformation to coordinates which are invariant under the S^1 action generated by C:

$$ix = 2w, \quad y = 2uv^*, \quad z = |u|^2 - |v|^2, \quad C = |u|^2 + |v|^2. \tag{1.15}$$

This is just the Hopf fibration in the (u,v) coordinates for $\mathbb{C}^2$. Physically, the variables x, y, and z represent the electric field, the polarization, and the population inversion, respectively. Transformation (1.15) gives us a five-dimensional system on the space $\mathbb{C}^2 \times \mathbb{R}$, coordinatized by (x, y, z). The Hamiltonian function, the Hamiltonian vector field for H, the equations of motion, and the new constants formed from those in (1.12) become

$$H = \frac{i}{2}(x^*y - xy^*), \tag{1.16}$$

$$\begin{aligned} X_H = {} & 2i\left(\frac{\partial H}{\partial x}\frac{\partial}{\partial x^*} - \frac{\partial H}{\partial x^*}\frac{\partial}{\partial x}\right) + 2iz\left(\frac{\partial H}{\partial y^*}\frac{\partial}{\partial y} - \frac{\partial H}{\partial y}\frac{\partial}{\partial y^*}\right) \\ & + iy\left(\frac{\partial H}{\partial y}\frac{\partial}{\partial z} - \frac{\partial H}{\partial z}\frac{\partial}{\partial y}\right) + iy^*\left(\frac{\partial H}{\partial z}\frac{\partial}{\partial y^*} - \frac{\partial H}{\partial y^*}\frac{\partial}{\partial z}\right), \end{aligned} \tag{1.17}$$

$$\dot{x} = y, \quad \dot{y} = xz, \quad \dot{z} = -\frac{1}{2}(x^*y + xy^*), \tag{1.18}$$

$$K = z + \frac{1}{2}|x|^2 \quad \text{and} \quad L = |y|^2 + z^2. \tag{1.19}$$

Physically, K is the sum of the atomic excitation energy and the electrical field energy, while $L = 1$, for unitarity. Fordy and Holm [1991] discuss the phase-space geometry of the solutions of the Maxwell-Bloch system (1.18) on $\mathbb{C}^2 \times \mathbb{R}$ and show that this system has *three* Hamiltonian structures, by using the Lax-pair representation of these equations.

In the remainder of this paper, we shall discuss the phase-space geometry and Hamiltonian structure of the invariant subsystem of (1.18) obtained by restricting to real-valued x and y. Thus, the dynamics of this invariant subsystem lie on the zero-level surface of the Hamiltonian function H in (1.16), with coordinates $x_1 = \mathrm{Re}(x)$, $x_2 = \mathrm{Re}(y)$, and $x_3 = z$. The equations of motion (1.18) then become the real Maxwell-Bloch equations,

$$\dot{x}_1 = x_2, \quad \dot{x}_2 = x_1x_3, \quad \dot{x}_3 = -x_1x_2. \tag{1.20}$$

Remark on Geometric Phases

Before discussing the phase-space geometry of the invariant subsystem (1.20) in detail, we remark that the values of the geometric phases in the reduced problem are not intrinsic; instead, they depend upon the choice of phase-space coordinates. This happens because the reduced motion takes place on symplectic leaves, which are the level sets of the constants of motion, and the choice of these constants of mo-

tion allows considerable freedom in phase-space parametrization. When reconstructing the solutions from the reduced system, especially for periodic solutions, phases are generated as a result of travelling over one period in the reduced space (in our case, on a level surface of C). These phases are associated with the group action of the reduction. Let M be a Poisson manifold on which G acts as a Hamiltonian Lie group of symmetry transformations with corresponding Lie algebra g, and let $C : M \to g^*$ be the associated momentum map. Then $P : M \to M_\mu = C^{-1}(\mu)/G_\mu$, the reduced space, has the structure of a vector bundle. (Here G_μ is the isotropy subgroup of μ.) For the S^1 reduction considered in the present case, the canonical 1-form

$$\Omega := \sum_i p_i dq_i = p\,dq + C\,d\varphi \tag{1.21}$$

may be taken as a connection on this bundle, where p and q are the symplectic coordinates for the level surface of C on which the reduced motion takes place. Relative to this connection, horizontal vector fields X_h satisfy $X_h \cdot \Omega = 0$. The *geometric phase* for a periodic orbit on the S^1-reduced phase space is obtained from the horizontal lift of the orbit (see Marsden et al. [1990]), Hence,

$$\Delta\varphi_{\text{geom}} = -\frac{1}{C}\oint_{\partial S} p\,dq = -\frac{1}{C}\int_S dp \wedge dq, \tag{1.22}$$

where the second equality uses Green's theorem (∂S denotes a periodic orbit on the reduced phase space, and S is the surface bounded by this orbit). For each of the reductions to symplectic motion on level surfaces of the Casimir functions C described in Sections 2 and 3, there is a corresponding geometric phase given by (1.22). In addition, the dynamical phase is defined by

$$\Delta\varphi_{\text{dyn}} = -\frac{1}{C}\oint_{\partial S} p_i\,dq_i = -\frac{1}{C}\int_{\partial S} (p\dot{q} + C\dot{\varphi})\,dt. \tag{1.23}$$

Naturally, the total phase is given by the sum of expressions (1.22) and (1.23). For Hamiltonian functions that are quadratic in each of the momenta, expression (1.23) adopts a particularly simple form,

$$\Delta\varphi_{\text{dyn}} = \frac{1}{C}\oint_{\partial S}\left(p\frac{\partial H}{\partial p} + C\frac{\partial H}{\partial C}\right)dt = \frac{1}{C}\oint_{\partial S} 2(H - V)\,dt = \frac{2T}{C}[H - \langle V\rangle] \tag{1.24}$$

where T is the period of the orbit on which the integration is performed and $\langle V\rangle$ denotes the average of the potential energy over the orbit. (See Montgomery [1991].)

Clearly, the values of $\Delta\varphi_{\text{geom}}$ and $\Delta\varphi_{\text{dyn}}$ depend upon the values of the functions H and C. However, the total phase, being a property of the orbit, is independent of any phase-space reparametrizations. In particular, for a given orbit ∂S, one could choose the value of H such that $\Delta\varphi_{\text{dyn}} = 0$, and the total phase (for that orbit) would then be completely geometrical.

In this introduction we have derived the complex Maxwell-Bloch system (1.18) and explained the embedding of the real-valued Maxwell-Bloch system (1.20) in $\mathbb{C}^3$. We have also discussed the geometric phases associated with reconstruction of the solutions on the unreduced space from those of the reduced system, and shown that the values of these phases are coordinate-dependent. The next section discusses the Hamiltonian structure of the real-valued system (1.20). For this system, a three-parameter family of Lie-Poisson Hamiltonian structures is introduced and labeled by SL(2, $\mathbb{R}$) parameters. Each Lie algebra characterizing these Lie-Poisson structures is associated with a particular symplectic foliation of $\mathbb{R}^3$ by level sets of a distinguished function, or Casimir function, associated with the center of the corresponding Lie algebra. In Section 3, equations (1.20) are explicitly reduced to two-dimensional completely integrable systems on the level sets of the Casimir functions. The bifurcations of the phase portraits on these level surfaces are also discussed. Finally, a summary of this work is presented in Section 4.

2. Classification of the Lie–Poisson Hamiltonian Structures for the Real-Valued Maxwell–Bloch System

As we have seen, the three-dimensional real-valued set of equations,

$$\dot{x}_1 = x_2, \quad \dot{x}_2 = x_1 x_3, \quad \dot{x}_3 = -x_1 x_2, \tag{1.20}$$

arises as an invariant subsystem of the Maxwell-Bloch equations for optical travelling-wave pulses in two-level media, a five (real) dimensional system on the space $\mathbb{C}^2 \times \mathbb{R}$. The latter system itself originates from the 2:1:1 resonant nonlinear oscillator system (1.10) on $\mathbb{C}^3$. Equations (1.20) are obtained as a result of restricting the space $\mathbb{C}^2 \times \mathbb{R}$ to $\mathbb{R}^3$ through restriction onto the zero-level surface of the Hamiltonian in $\mathbb{C}^2 \times \mathbb{R}$. Equations (1.20) also appear as the large Rayleigh number limit of the famous Lorenz system (see Sparrow [1982]).

Equations (1.20) are expressible in three-dimensional vector notation as

$$\dot{x} = \nabla H_1 \times \nabla H_2, \tag{2.1}$$

where H_1 and H_2 are the two conserved functions

$$\begin{aligned} H_1 &= \frac{1}{2}(x_2^2 + x_3^2), \\ H_2 &= x_3 + \frac{1}{2}x_1^2. \end{aligned} \tag{2.2}$$

Equation (2.1) implies a local rectification of the flow into $(\dot{y}_1, \dot{y}_2, \dot{y}_3) = (0, 0, 1)$, obtained by choosing $y_1 = H_1$ and $y_2 = H_2$. In this work, however, we are interested in the global geometry of the flow.

Geometrically, equation (2.1) implies that the motion takes place on intersections of level sets of the functions H_1 and H_2 in the space $\mathbb{R}^3$. Poisson flows on the dual g^* of a three-dimensional Lie algebra g (isomorphic to $\mathbb{R}^3$) have a Lie-Poisson structure

$$X_H \cdot F(x) = \{F, H\}(x) = \langle x, [\nabla F, \nabla H] \rangle, \tag{2.3}$$

where $F, H : g^* \to \mathbb{R}, g \sim g^{**}, \nabla F, \nabla H \in g$, and $x \in g^*$, with the (canonical) pairing $\langle \cdot, \cdot \rangle : g^* \times g \to \mathbb{R}$ and Lie bracket $[\cdot, \cdot]$ on g. Such flows are expressible in the form (2.1) whenever the algebra g has a nontrivial center. These flows comprise a subclass of the integrable divergenceless flows on $\mathbb{R}^3$ (see Holm and Kimura [1991]). Equation (2.1) also implies that the system is bi-Hamiltonian; since either of H_1 and H_2 can be used as a Hamiltonian function, the second function plays the role of a Casimir (or a distinguished) function. The compatibility of these two Hamiltonian structures is obvious; just replace ∇H_1 by $\nabla(H_1 + H_2)$ in (2.1). Equations (2.1) may be re-expressed as

$$\dot{x} = \nabla H \times \nabla C, \tag{2.4}$$

where H and C are SL(2, $\mathbb{R}$) combinations of H_1 and H_2. Namely,

$$\begin{bmatrix} H \\ C \end{bmatrix} = \begin{bmatrix} \alpha & \beta \\ \mu & \nu \end{bmatrix} \begin{bmatrix} H_1 \\ H_2 \end{bmatrix}, \tag{2.5}$$

with $\alpha\nu - \beta\mu = 1$.

Proposition. Consider the two functions $H = \alpha H_1 + \beta H_2, C = \mu H_1 + \nu H_2$, with $\alpha\nu - \beta\mu = 1$. Then equations (2.1) are equivalent to (2.4). For the proof, it suffices to compute

$$\begin{aligned} \dot{x} &= \nabla H \times \nabla C = \nabla(\alpha H_1 + \beta H_2) \times \nabla(\mu H_1 + \nu H_2) = (\alpha\nu - \beta\mu)\nabla H_1 \times \nabla H_2 \\ &= \nabla H_1 \times \nabla H_2. \end{aligned} \tag{2.6}$$

Thus, the real-valued Maxwell-Bloch equations (1.20) are unchanged (so the trajectories of the motion in $\mathbb{R}^3$ remain the same) when the conserved functions H_1 and H_2 are replaced by the SL(2, $\mathbb{R}$) combinations H and C. (Taking SL(2, $\mathbb{R}$) linear combinations is a slight extension of the idea of homotopy.) Geometrically, the invariance of the trajectories in $\mathbb{R}^3$ means that while the level surfaces of H and C may be radically different from those of H_1 and H_2, their intersections are exactly the same.

This proposition implies invariance of the intersections of level surfaces of the functions H and C under the SL(2, $\mathbb{R}$) group action (2.5), so that the dynamics remains unchanged, in particular that the geometric loci of the solutions are invariant under (2.5).

Let us now examine the Lie-Poisson structure of our system. Because of the invariance of (2.1) under the above action of SL(2, $\mathbb{R}$), this structure will not be unique. Here, we adopt Hamiltonian vector fields as our basic working objects; the correspondence with Poisson brackets is given through the following identity

$$X_H F = -X_F H = \{F, H\}. \tag{2.7}$$

The equations governing the flow of X_H are the Hamiltonian equations for H. The set of Hamiltonian vector fields satisfies the same algebra as that specified by the bracket, up to an anti-isomorphism:

$$X_{\{F,H\}} = [X_H, X_F]. \tag{2.8}$$

In view of (2.1) it is then clear that for functions $G : \mathbb{R}^3 \to \mathbb{R}$, we have

$$X_G = (\nabla G \times \nabla C) \cdot \nabla. \tag{2.9}$$

In component form, this is expressed as

$$\begin{aligned} X_G = {} & (\nu + \mu x_3)\left(\frac{\partial G}{\partial x_2}\frac{\partial}{\partial x_1} - \frac{\partial G}{\partial x_1}\frac{\partial}{\partial x_2}\right) + \nu x_1\left(\frac{\partial G}{\partial x_3}\frac{\partial}{\partial x_2} - \frac{\partial G}{\partial x_2}\frac{\partial}{\partial x_3}\right) \\ & + \mu x_2\left(\frac{\partial G}{\partial X_1}\frac{\partial}{\partial x_3} - \frac{\partial G}{\partial x_3}\frac{\partial}{\partial x_1}\right), \end{aligned} \tag{2.10}$$

and any dynamical quantity Q evolves with time according to

$$\dot{Q} = X_H Q. \tag{2.11}$$

We note that expression (2.10) exhibits an explicit dependence on the parameters μ and ν, through its dependence on the distinguished function C, as prescribed in the Proposition. Naturally, the Hamiltonian function H also contains parameters α and β, with the proviso that $\alpha\nu - \beta\mu = 1$.

In order to determine the structure of the Lie algebra underlying the Poisson structure, we calculate the Lie bracket for the Hamiltonian vector fields associated with the coordinate functions x_i,

$$\begin{aligned} X_1 := X_{x_1} &= \mu x_2 \partial_3 - (\nu + \mu x_3)\partial_2, \\ X_2 := X_{x_2} &= (\nu + \mu x_3)\partial_1 - \nu x_1 \partial_3, \\ X_3 := X_{x_3} &= \nu x_1 \partial_2 - \mu x_2 \partial_1, \end{aligned} \tag{2.12}$$

where $\partial_i = \partial/\partial x_i$. The commutators are found to be

$$[X_1, X_2] = -\mu X_3, \quad [X_2, X_3] = -\nu X_1, \quad [X_3, X_1] = -\mu X_2. \tag{2.13}$$

It is clear that the Lie algebra spanned by the X_i depends on μ and ν. The type of dependence is correlated with the type of orbits in the group SL(2, $\mathbb{R}$). Thus, three cases can arise.

Case 1. $\mu = 0, \nu \neq 0$. Let us define $Y_1 = -\nu X_1, Y_2 = X_2, Y_3 = X_3$. Then the structure of the algebra is

$$[Y_1, Y_2] = 0, \quad [Y_2, Y_3] = Y_1, \quad [Y_3, Y_1] = 0. \tag{2.14}$$

This algebra is of type II in Bianchi's classification (see, e.g., Dubrovin et al. [1982]). It is solvable and is identified with the well-known Heisenberg algebra.

Case 2. $\mu \neq 0, \nu = 0$. Let us define $Y_1 = -X_1/\mu, Y_2 = X_2, Y_3 = X_3$. Then the structure of the algebra is

$$[Y_1, Y_2] = Y_3, \quad [Y_2, Y_3] = 0, \quad [Y_3, Y_1] = Y_2. \tag{2.15}$$

This solvable algebra is of type VII in Bianchi's classification and is isomorphic to the Euclidean algebra of the plane.

Case 3. $\mu \neq 0 = \epsilon_\mu$, $\nu \neq 0 = \epsilon_\nu$, where $\epsilon_\sigma = \text{Sign}(\sigma)$. Let us define a new basis $Y_1 = -\epsilon_\nu X_1/|\mu|$, $Y_2 = X_2/(|\mu||\nu|)^{1/2}$, $Y_3 = X_3/(|\mu||\nu|)^{1/2}$. Then the structure of the algebra is

$$[Y_1, Y_2] = \epsilon Y_3, \quad [Y_2, Y_3] = Y_1, \quad [Y_3, Y_1] = \epsilon Y_2. \tag{2.16}$$

where $\epsilon = \epsilon_{\mu\nu} = \text{Sign}(\mu\nu)$. Two subcases arise.

Subcase 3.1. $\epsilon = 1$. This algebra is of type IX in Bianchi's classification and isomorphic to so(3).

Subcase 3.2. $\epsilon = -1$. This algebra is of type VIII in Bianchi's classification and isomorphic to so(2,1) and so(1,2).

Each of the above cases is associated with particular class of Casimir functions C.

Case 1. $\mu = 0$, $\nu \neq 0$. The level sets of C are parabolic cylinders along the x_2-axis (see Figure 2.1),

$$C = \nu\left(x_3 + \frac{1}{2}x_1^2\right). \tag{2.17}$$

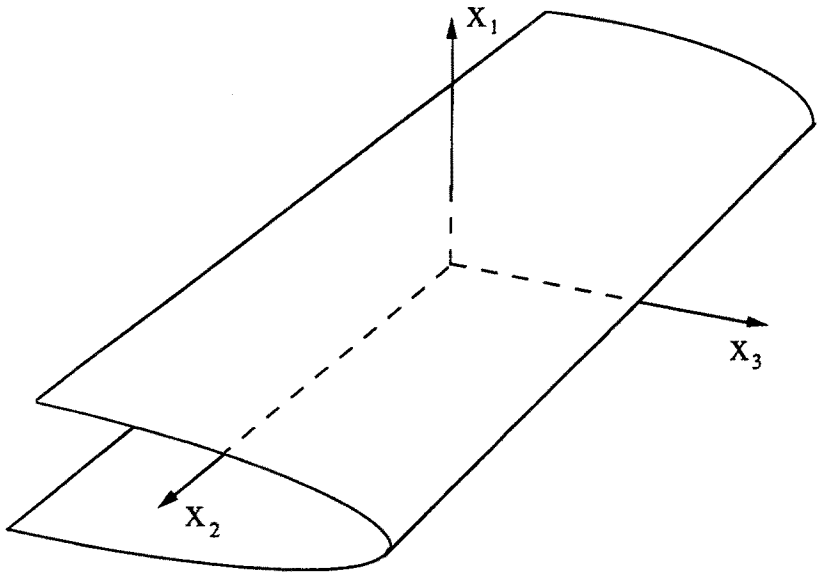

Fig. 2.1. The level sets of C for Case 1.

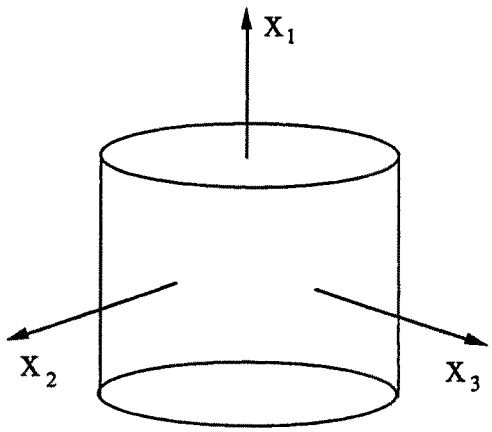

Fig. 2.2. The level sets of C for Case 2.

Case 2. $\mu \neq 0, \nu = 0$. For this second case, the level sets are circular cylinders about the x_1-axis (see Figure 2.2), defined whenever $C/\mu > 0$,

$$C = \frac{1}{2}\mu\left(x_2^2 + x_3^2\right). \tag{2.18}$$

Case 3a. $\mu \neq 0, \nu \neq 0$, with $\mu\nu > 0$. The level sets are ellipsoids of revolution (see Figure 2.3), with semimajor axis $r_1 = r, r_2 = r_3 = (\nu/\mu)^{1/2}r$, centered at

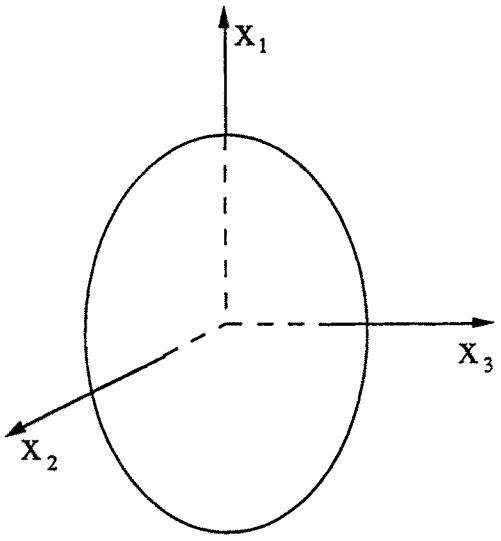

Fig. 2.3. The level sets of C for Case 3a.

$(0, 0, -\nu/\mu)$; they are defined whenever $4\mu C + \nu^2 > 0$.

$$x_1^2 + \frac{\mu}{\nu}\left[x_2^2 + \left(x_3 + \frac{\nu}{\mu}\right)^2\right] = \frac{2C}{\nu} + \frac{\nu}{2\mu} =: r^2 \tag{2.19}$$

Case 3b. $\mu \neq 0, \nu \neq 0$, with $\mu\nu < 0$. The level sets, here, are noncompact surfaces. They are two-sheeted hyperboloids of revolution if $4\mu C + \nu^2 < 0$, one-sheeted hyperboloids if $4\mu C + \nu^2 > 0$, and a cone whenever $4\mu C + \nu^2 = 0$ (see Figure 2.4). The two varieties of hyperboloids correspond to the two choices of the algebra, either so(2,1) or so(1,2).

We end this section by mentioning that each of the above classes, in addition to giving us a type for the function C, also gives a prescription for the Hamiltonian function H. In fact, the admissible pairs (H, C) are prescribed by (2.5) where the matrices of $SL(2, \mathbb{R})$ are respectively given as follows:

$$\begin{aligned}
&\text{Case 1}: g_1 = \begin{bmatrix} 1/\nu & \beta \\ 0 & \nu \end{bmatrix}, && H = \frac{H_1}{\nu} + \beta H_2, \\
&\text{Case 2}: g_2 = \begin{bmatrix} \alpha & -1/\mu \\ \mu & 0 \end{bmatrix}, && H = \alpha H_1 - \frac{H_2}{\mu}, \\
&\text{Case 3}: g_3 = \begin{bmatrix} \alpha & \beta \\ \mu & \nu \end{bmatrix}, && H = \alpha H_1 + \beta H_2, \quad \alpha\nu - \beta\mu = 1, \quad \mu\nu \neq 0.
\end{aligned} \tag{2.20}$$

In any of these cases, the locus of the Hamiltonian function H depends on the parameters α or β; therefore, it is not unique. Indeed, bifurcations can occur as we vary the parameters. For instance, a change in sign may change a level surface of energy from an ellipsoid to a hyperboloid. Remarkably, the intersection of the level surfaces of C and H do not see these bifurcations; in fact, they do not depend on the parameters at all. However, the *representation* of the dynamics *does* depend on the choice of parameters, as will be made explicit in the next section where we show, for example, that $\beta = 0$ in Case 1 yields Duffing oscillator dynamics, while $\alpha = 0$ in Case 2 yields pendulum dynamics.

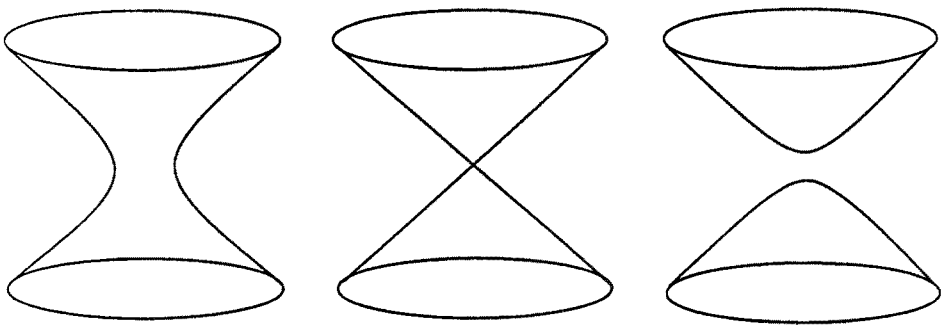

Fig. 2.4. The level sets of C for Case 3b.

3. Reductions to the Two-dimensional Level Sets of the Distinguished Functions

As mentioned previously, each of the cases presented in Section 2 yields a distinct reduction of the real-valued Maxwell-Bloch system (1.20) to a symplectic system on a two-dimensional manifold specified by a level set of the corresponding Casimir function C. The various reductions give different coordinate representations of the *same* solutions in $\mathbb{R}^3$. We discuss each reduction and give the prescription for the reduced phase spaces. For more details about the nature and technique used to perform reduction, the reader is referred, for example, to Abraham and Marsden [1978], or Section 6.3 in Olver [1986].

Case 1. $\mu = 0, \nu \neq 0$. The Casimir function C is given by (2.17), and the Hamiltonian function is, as prescribed by (2.2) and the proposition following (2.5),

$$H = \frac{1}{2\nu}(x_2^2 + x_3^2) + \beta\left(x_3 + \frac{1}{2}x_1^2\right). \tag{3.1}$$

We show that this system reduces to the Duffing oscillator. To that end, we introduce a new basis of coordinate functions; it is natural to choose them as

$$\begin{aligned} x &= x_1, & x_1 &= x, \\ y &= x_2, & x_2 &= y, \\ z &= x_3 + \frac{1}{2}x_1^2, & x_3 &= z - \frac{1}{2}x^2. \end{aligned} \tag{3.2}$$

In terms of these coordinates, the functions C and H become

$$\begin{aligned} C &= \nu z, \\ H &= \beta z + \frac{y^2 + (z - x^2/2)^2}{2\nu}. \end{aligned} \tag{3.3}$$

Thus, level sets of the Hamiltonian function are biquadratic surfaces. Associated with the transformation (3.2), the basis of the tangent space becomes

$$\partial_1 = \partial_x + x\partial_z, \quad \partial_2 = \partial_y, \quad \partial_3 = \partial_z. \tag{3.4}$$

The Hamiltonian vector field and the equations of the motion therefore reduce to

$$X_H = \nu\left(\frac{\partial H}{\partial y}\frac{\partial}{\partial x} - \frac{\partial H}{\partial x}\frac{\partial}{\partial y}\right), \tag{3.5}$$

$$\dot{x} = y, \quad \dot{y} = \left(z - \frac{1}{2}x^2\right)x, \quad z = \text{const.} \tag{3.6}$$

This system is a Duffing oscillator and it possesses the following three critical points: $(x, y) = (0, 0), (\pm\sqrt{2z}, 0)$. The first of these is unstable, and the two others are stable centers (see Figure 3.1).

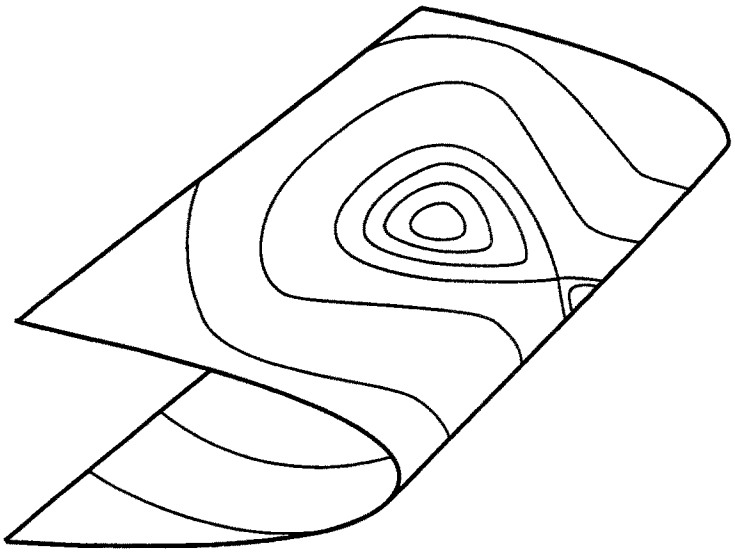

Fig. 3.1. Duffing type reduced phase space for Case 1.

Case 2. $\mu \neq 0$, $\nu = 0$. For this case, the Casimir function C is given by (2.18) and the Hamiltonian function is

$$H = \frac{\alpha}{2}(x_2^2 + x_3^2) - \frac{1}{\mu}\left(x_3 + \frac{1}{2}x_1^2\right). \tag{3.7}$$

We introduce a new basis of coordinate functions. Since the level sets of C are circular cylinders, it is natural to choose the usual cylindrical coordinates,

$$x_1 = z, \quad x_2 = rC_\theta, \quad x_3 = rS_\theta, \quad r = \sqrt{\frac{2C}{\mu}} \tag{3.8}$$

where we have defined $C_\theta := \cos(\theta)$ and $S_\theta := \sin(\theta)$; we will use this notation from here on, together with $Ch_u := \cosh(u)$ and $Sh_u := \sinh(u)$. In terms of these coordinates, the Casimir and Hamiltonian functions become

$$\begin{aligned} C &= \frac{\mu r^2}{2}, \\ H &= \frac{1}{\mu}\left(\alpha C - \frac{1}{2}z^2 - rS_\theta\right). \end{aligned} \tag{3.9}$$

For this second case, the level sets of the Hamiltonian are parabolic cylinders along the x_2-axis. The orbits of the motion are the intersections of these parabolic cylinders with a circular cylinder about the z-axis (see Figure 3.2). These intersections are nontrivial only when $\mu H - \alpha C < r$. Therefore, the orbits on the phase cylinder are periodic, except in the limit when one of the parabolic cylinders becomes tangent with the interior of the circular cylinder; when this occurs, a pair of homoclinic loops appears which partitions the phase cylinder into three distinct families of periodic

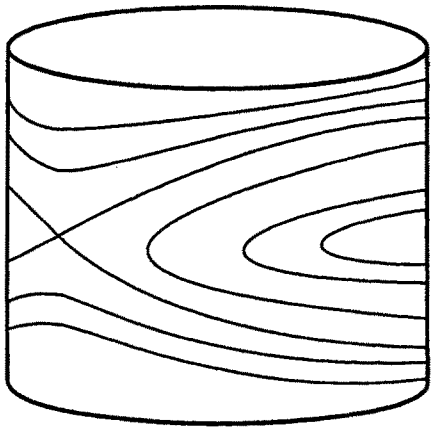

Fig. 3.2. Phase portrait for Case 2.

orbits. The transformation of basis in the tangent space induced by (3.8) is

$$\begin{aligned} \partial_1 &= \partial_z, \\ \partial_2 &= C_\theta \partial_r - \frac{1}{r} S_\theta \partial_\theta, \\ \partial_3 &= S_\theta \partial_r + \frac{1}{r} S_\theta \partial_\theta. \end{aligned} \tag{3.10}$$

The Hamiltonian vector field X_H reduces to

$$X_H = \mu \left(\frac{\partial H}{\partial z} \frac{\partial}{\partial \theta} - \frac{\partial H}{\partial \theta} \frac{\partial}{\partial z} \right), \tag{3.11}$$

so that the reduced equations of motion are

$$\dot{\theta} = -z, \qquad \dot{z} = rC_\theta, \quad r = \text{const.} \tag{3.12}$$

Thus, in these coordinates, the motion on the reduced phase cylinder reduces to pendulum dynamics (see Figure 3.2).

Case 3a. $\mu \neq 0, \nu \neq 0, \mu\nu > 0, 4\mu C + \nu^2 > 0$. For this third case, the Casimir function C is given by expression (2.19). Introducing the constant

$$r = \sqrt{\frac{2C}{\nu} + \frac{\nu}{2\mu}}, \tag{3.13}$$

and recalling that the level sets of the Casimir function are ellipsoids of revolution about the x_1-axis, suggests introducing a new basis of coordinate functions as follows

$$
\begin{aligned}
x_1 &= rC_\theta, \\
x_2 &= \sqrt{\frac{\nu}{\mu}} rS_\theta C_\varphi, \\
x_3 &= -\frac{\nu}{\mu} + \sqrt{\frac{\nu}{\mu}} rS_\theta S_\varphi.
\end{aligned} \tag{3.14}
$$

In terms of these coordinates (upon using $\alpha\nu - \beta\mu = 1$), the Casimir and Hamiltonian functions become

$$
\begin{aligned}
C &= \frac{2\mu^2 r^2 - \nu^2}{4\mu}, \\
H &= \frac{\nu(2 - \alpha\nu) + \alpha\mu\nu r^2}{2\mu^2} - \frac{r^2 C_\theta^2}{2\mu} - \sqrt{\frac{\nu}{\mu}} \frac{r}{\mu} S_\theta S_\varphi.
\end{aligned} \tag{3.15}
$$

Thus, a level set of C is a displaced sphere of radius r. Notice that all the α- and β-dependence in the Hamiltonian is confined to the constant term. This implies that the equations of the motion, in contrast, will exhibit no dependence whatsoever on these two parameters. The geometric significance is that the orbits of the motion are invariant under SL(2, $\mathbb{R}$) deformations of the functions C and H. Under the change of coordinate functions (3.14), the basis of vector fields is expressed as

$$
\begin{aligned}
\partial_1 &= C_\theta \partial_r - \frac{1}{r} S_\theta \partial_\theta, \\
\partial_2 &= \sqrt{\frac{\mu}{\nu}} \left[S_\theta C_\varphi \partial_r + \frac{1}{r} C_\theta C_\varphi \partial_\theta - \frac{S_\varphi}{rS_\theta} \partial_\varphi \right], \\
\partial_3 &= \sqrt{\frac{\mu}{\nu}} \left[S_\theta S_\varphi \partial_r + \frac{1}{r} C_\theta S_\varphi \partial_\theta + \frac{C_\varphi}{rS_\theta} \partial_\varphi \right].
\end{aligned} \tag{3.16}
$$

The Hamiltonian vector field then becomes

$$
X_H = \frac{\mu}{rS_\theta} \left(\frac{\partial H}{\partial \varphi} \frac{\partial}{\partial \theta} - \frac{\partial H}{\partial \theta} \frac{\partial}{\partial \varphi} \right), \tag{3.17}
$$

and the equations of the motion are

$$
\begin{aligned}
\dot{\theta} &= -\sqrt{\frac{\nu}{\mu}} C_\varphi, \\
\dot{\varphi} &= -\frac{C_\theta}{S_\theta} \left(rS_\theta - \sqrt{\frac{\nu}{\mu}} S_\varphi \right).
\end{aligned} \tag{3.18}
$$

These equations admit up to four distinct critical points, $(\theta, \varphi) = (\pi/2, \pm\pi/2)$, as well as the pair $(S_\theta, \varphi) = [(\nu/\mu r^2)^{1/2}, \pi/2]$; the latter exist whenever $r > \sqrt{\nu/\mu}$. A simple linear stability analysis provides us with the following information. The points $(\theta, \varphi) = (\pi/2, -\pi/2)$ and $(S_\theta, \varphi) = [(\nu/\mu r^2)^{1/2}, \pi/2]$ are always stable. As for $(\theta, \varphi) = (\pi/2, \pi/2)$, this point is stable if $r < \sqrt{\nu/\mu}$ and is of saddle type

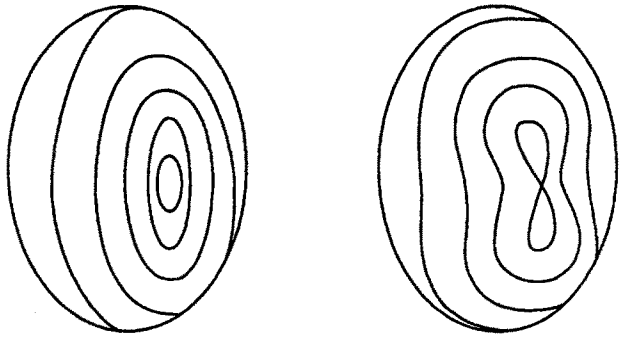

Fig. 3.3. Phase portraits for Case 3a.

whenever $r > \sqrt{\nu/\mu}$. Therefore, a Hamiltonian pitchfork bifurcation takes place at $r = \sqrt{\nu/\mu}$, i.e., when $4\mu C - \nu^2 = 0$ (see Figure 3.3). We mention that such a bifurcation did not occur for the previous case. Indeed, referring to Figure 3.2, it is clear that both of the two homoclinic loops are forbidden to shrink to a point on the cylinder.

Case 3b. $\mu \neq 0$, $\nu \neq 0$, $\mu\nu < 0$. For this last case, the Casimir function C is given by a hyperbolic quadric. Thus, we must consider subcases corresponding to the three possible geometries of the level sets of the Casimir function,

$$x_1^2 + \frac{\mu}{\nu}\left[x_2^2 + \left(x_3 + \frac{\nu}{\mu}\right)^2\right] = \frac{4\mu C + \nu^2}{2\mu\nu} =: R. \tag{3.19}$$

Subcase 3b.1. $4\mu C + \nu^2 < 0$. Then $R = r^2 > 0$. For this first subcase, level sets of the Casimir function are two-sheeted hyperboloids. A natural set of new coordinate functions is provided by (recall that we defined $Ch_u = \cosh(u)$ and $Sh_u = \sinh(u)$).

$$\begin{aligned} x_1 &= rCh_u, \\ x_2 &= \sqrt{\frac{-\nu}{\mu}}rSh_uC_\varphi, \\ x_3 &= -\frac{\nu}{\mu} + \sqrt{\frac{-\nu}{\mu}}rSh_uS_\varphi. \end{aligned} \tag{3.20}$$

In terms of these coordinates, the Casimir function and the Hamiltonian function take the forms

$$\begin{aligned} C &= \frac{2\mu\nu r^2 - \nu^2}{4\mu}, \\ H &= \frac{\nu(2-\alpha\nu) + \alpha\mu\nu r^2}{2\mu^2} - \frac{r^2Ch_u^2}{2\mu} - \sqrt{-\frac{\nu}{\mu}}\frac{r}{\mu}Sh_uS_\varphi. \end{aligned} \tag{3.21}$$

Again, only the constant term of the Hamiltonian function shows any dependence on the parameter α; the geometry of the solutions in the unreduced phase space $\mathbb{R}^3$ is therefore blind to this parameter. The transformation in the tangent space is

$$\begin{aligned}
\partial_1 &= Ch_u\partial_r - \frac{1}{r}Sh_u\partial_u, \\
\partial_2 &= \sqrt{-\frac{\mu}{\nu}}\left[-Sh_uC_\varphi\partial_r + \frac{1}{r}Ch_uC_\varphi\partial_u + \frac{S_\varphi}{rSh_u}\partial_\varphi\right], \\
\partial_3 &= \sqrt{\frac{-\mu}{\nu}}\left[Sh_uS_\varphi\partial_r - \frac{1}{r}Ch_uS_\varphi\partial_u + \frac{C_\varphi}{rSh_u}\partial_\varphi\right].
\end{aligned} \tag{3.22}$$

The Hamiltonian vector field then reduces to

$$X_H = \frac{\mu}{rSh_u}\left(\frac{\partial H}{\partial u}\frac{\partial}{\partial \varphi} - \frac{\partial H}{\partial \varphi}\frac{\partial}{\partial u}\right), \tag{3.23}$$

so that the equations of the motion on the reduced space are

$$\dot{u} = \sqrt{\frac{-\nu}{\mu}}C_\varphi, \qquad \dot{\varphi} = \frac{-Ch_u}{Sh_u}\left(rSh_u + \sqrt{\frac{-\nu}{\mu}}S_\varphi\right). \tag{3.24}$$

These equations possess two critical points, $(\varphi, Sh_u) = (\pi/2, -\sqrt{-\nu/\mu}/r)$ on the bottom sheet of the hyperboloid, and $(\varphi, Sh_u) = (-\pi/2, \sqrt{-\nu/\mu}/r)$ on the top sheet. Both of these critical points are stable. Thus, each sheet of the hyperboloidal reduced space is foliated by a family of periodic orbits (see Figure 3.4).

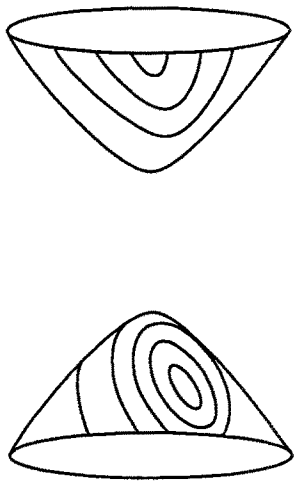

Fig. 3.4. Phase portraits for Case 3b.1.

Remark. The Hamiltonian (3.21) is invariant under the $\mathbb{Z}_2$ action $(u, \varphi) \to (-u, -\varphi)$. We could use that symmetry to further reduce the system to a single hyperboloidal sheet. (The phase present is invariant under the above transformation, except for a reversal of the time flow.)

Subcase 3b.2. $4\mu C + \nu^2 > 0$. Then $R = -r^2 > 0$. For this second subcase, level sets of the Casimir function C are one-sheeted hyperboloids. We choose new coordinate functions as follows:

$$\begin{aligned} x_1 &= rSh_u, \\ x_2 &= \sqrt{\frac{-\nu}{\mu}} rCh_u C_\varphi, \\ x_3 &= -\frac{\nu}{\mu} + \sqrt{\frac{-\nu}{\mu}} rCh_u S_\varphi. \end{aligned} \tag{3.25}$$

In terms of these, the distinguished function C and the Hamiltonian function H become

$$\begin{aligned} C &= \frac{-(2\mu\nu r^2 + \nu^2)}{4\mu}, \\ H &= \frac{\nu(2 - \alpha\nu) - \alpha\mu\nu r^2}{2\mu^2} - \frac{r^2 Sh_u^2}{2\mu} - \sqrt{\frac{-\nu}{\mu}} \frac{r}{\mu} Ch_u S_\varphi. \end{aligned} \tag{3.26}$$

The tangent space vector fields are then transformed according to

$$\begin{aligned} \partial_1 &= -Sh_u \partial_r + \frac{1}{r} Ch_u \partial_u, \\ \partial_2 &= \sqrt{\frac{-\mu}{\nu}} \left[Ch_u C_\varphi \partial_r - \frac{1}{r} Sh_u C_\varphi \partial_u - \frac{S_\varphi}{rCh_u} r\partial_\varphi \right], \\ \partial_3 &= \sqrt{\frac{-\mu}{\nu}} \left[Ch_u S_\varphi \partial_r - \frac{1}{r} Sh_u S_\varphi \partial_u + \frac{C_\varphi}{rCh_u} r\partial_\varphi \right]. \end{aligned} \tag{3.27}$$

The Hamiltonian vector field then reduces to

$$X_H = \frac{\mu}{rCh_u} \left(\frac{\partial H}{\partial u} \frac{\partial}{\partial \varphi} - \frac{\partial H}{\partial \varphi} \frac{\partial}{\partial u} \right), \tag{3.28}$$

and the equations of the motion are consequently

$$\begin{aligned} \dot{u} &= \sqrt{\frac{-\nu}{\mu}} C_\varphi, \\ \dot{\varphi} &= \frac{-Sh_u}{Ch_u} \left(rCh_u + \sqrt{\frac{-\nu}{\mu}} S_\varphi \right). \end{aligned} \tag{3.29}$$

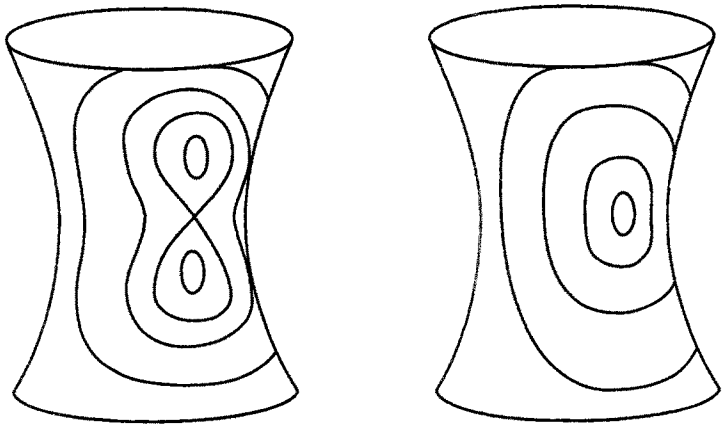

Fig. 3.5. Phase portraits for Case 3b.2.

These equations admit up to four fixed points, $(u, \varphi) = (0, \pm\pi/2)$, as well as the pair $(Ch_u, \varphi) = [\pm(\nu/\mu r^2)^{1/2}, -\pi/2]$; the latter exist whenever $r < \sqrt{-\nu/\mu}$. Linear stability analysis provides us with the following information. The points $(u, \varphi) = (0, \pi/2)$ and $(Ch_u, \varphi) = [\pm(\nu/\mu r^2)^{1/2}, -\pi/2]$ are always stable. As for $(u, \varphi) = (0, -\pi/2)$, this point is stable if $r > \sqrt{-\nu/\mu}$ and is of saddle type whenever $r < \sqrt{-\nu/\mu}$. Therefore we have the phase portraits of Figure 3.5.

Subcase 3b.3. $4\mu C + \nu^2 = 0$. Then $R = 0$. For this last case, the level sets of the Casimir functions C are cones. To restrict to the conical level sets, we choose new coordinate functions as follows:

$$\begin{aligned} x_1 &= z, \\ x_2 &= \sqrt{\frac{-\nu}{\mu}} z C_\varphi, \\ x_3 &= -\frac{\nu}{\mu} + \sqrt{\frac{-\nu}{\mu}} z S_\varphi, \end{aligned} \tag{3.30}$$

which are singular at the vertex of the cone, $z = 0$. In terms of these, the distinguished function C and the Hamiltonian function H become

$$C = \frac{-\nu^2}{4\mu}, \qquad H = \frac{\nu(2 - \alpha\nu)}{2\mu^2} - \sqrt{\frac{-\nu}{\mu}} \frac{z}{\mu} S_\varphi - \frac{z^2}{2\mu}. \tag{3.31}$$

Once more, we note that the α-dependence of the Hamiltonian function is only within the constant term, so that it does not affect the dynamics, as far as the nature of the solution is concerned. The tangent space vector fields are then transformed according to

$$\begin{aligned}
\partial_1 &= \partial_z, \\
\partial_2 &= \sqrt{\frac{-\mu}{\nu}}\left[C_\varphi \partial_z - \frac{1}{z} S_\varphi \partial_\varphi\right], \\
\partial_3 &= \sqrt{\frac{-\mu}{\nu}}\left[S_\varphi \partial_z + \frac{1}{z} C_\varphi \partial_\varphi\right].
\end{aligned} \tag{3.32}$$

The Hamiltonian vector field then reduces to

$$X_H = 2\mu\left(\frac{\partial H}{\partial z}\frac{\partial}{\partial \varphi} - \frac{\partial H}{\partial \varphi}\frac{\partial}{\partial z}\right), \tag{3.33}$$

and the equations of the motion are

$$\begin{aligned}
\dot{z} &= 2\sqrt{\frac{-\nu}{\mu}} z C_\varphi, \\
\dot{\varphi} &= -2\left(z + \sqrt{\frac{-\nu}{\mu}} S_\varphi\right).
\end{aligned} \tag{3.34}$$

These equations possess three fixed points. One of them is $(z, \varphi) = (0, 0) = (0, \pi)$; this is really a single point, located at the vertex of the cone. The two other critical points are $(z, \varphi) = (-\sqrt{-\nu/\mu}, \pi/2), (\sqrt{-\nu/\mu}, -\pi/2)$. Linear stability analysis shows that the latter are always stable, while the point at the vertex of the cone is an unstable point. The nature of the phase portrait is as follows (see Figure 3.6). Two homoclinic orbits are connected to $z = 0$, one on each half of the cone; these separate the halves into two regions foliated by a family of periodic orbits.

Note: This case also has a $\mathbb{Z}_2$ symmetry, $(z, \varphi) \to (-z, -\varphi)$ which would allow us to reduce the phase space further to a single branch of the cone.

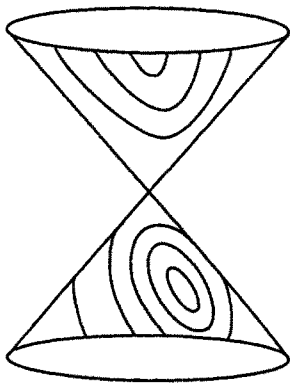

Fig. 3.6. Types of portraits for Case 3b.3.

4. Conclusion

In this paper, we have investigated the three-dimensional real-valued Maxwell-Bloch equations. Invariance of these equations under the action of the Lie group SL(2, $\mathbb{R}$) on the space of Hamiltonians has provided a classification of the various Lie-Poisson structures admitted by the system. Each structure is associated with a distinct Hamiltonian reduction, due to an S^1 invariance, on a quadratic surface defined as a level set of the second Hamiltonian function (which is also a Casimir function for the corresponding Lie-Poisson structure) embedded in $\mathbb{R}^3$ as a phase space for a one-degree-of-freedom system. On the reduced symplectic space, the motion is coordinate-dependent; for example, the reduced dynamics may be expressed as either that of a pendulum, or that of a Duffing oscillator, depending upon the choice of Casimir functions. This coordinate dependence has been used to seek the simplest representation of the solutions, as well as to illuminate the geometry of the bifurcations that occur. The various reductions give different values of the geometric phases for the Maxwell-Bloch solutions, depending upon on the choice of the Casimir function used to define a horizontal lift from the reduced symplectic space to the full phase space.

Clearly, the same SL(2, $\mathbb{R}$) invariance holds for any system expressible in the form (2.1). When H_1 and H_2 are quadratic, the Hamiltonian structure is Lie-Poisson. However, the SL(2, $\mathbb{R}$) invariance of the dynamics in $\mathbb{R}^3$ holds for nonquadratic Hamiltonians, as well. This invariance may be useful in other situations for seeking the simplest geometric representations of the phase trajectories as intersections of level surfaces of H and C in $\mathbb{R}^3$. For example, Holm and Marsden [1991] use this SL(2, $\mathbb{R}$) invariance to reduce the dynamics of a rigid body with controlled feedback torque to the classical simple pendulum equations.

Acknowledgments

We are grateful to R. B. Gardner, P. S. Krishnaprasad, J. E. Marsden, and W. Shadwick for helpful comments and discussions of this work.

References

R. Abraham and J. E. Marsden [1978] *Foundations of Mechanics*, Reading, MA: Benjamin/Cummings.

L. Allen and J. H. Eberly [1987] *Optical Resonance and Two-level Atoms*, New York: Dover.

B. A. Dubrovin, S. P. Novikov, and A. T. Fomenko [1984] *Modern Geometry—Methods and Applications*, Graduate Texts in Mathematics, Volume 93, New York: Springer-Verlag.

A. Fordy and D. D. Holm [1991] A tri-Hamiltonian formulation of the self-induced transparency equations, *Phys. Lett. A* **160**, 143–148.

D. D. Holm and Y. Kimura [1991] Zero-helicity Lagrangian kinematics of three-dimensional advection, *Phys. Fluids A* **3** (5), 1033–1038.

D. D. Holm and G. Kovacic [1991] Homoclinic chaos in a laser-matter system, Los Alamos preprint LA-UR-91-1300, Physica D (in press).

D. D. Holm and J. E. Marsden [1991] The Rotor and the Pendulum, in *Symplectic Geometry and Mathematical Physics*, edited by P. Donato, C. Duval, J. Elhadad, and G. M. Tuynman, Progress in Mathematics, Vol. 99, Bilkhauser: Boston, pp. 189–203.

J. E. Marsden, R. Montgomery, and T. Ratiu [1991] Reduction, symmetry, and Berry's phase in mechanics, *Mem. AMS*, **88**.

R. Montgomery [1991] How much does the rigid body rotate? A Berry's phase from the 18th Century, *Am. J. Phys.* **59**, 394–398.

P. J. Olver [1986] *Applications of Lie Groups to Differential Equations*, Graduate Texts in Mathematics 107, New York: Springer-Verlag.

G. P. Puccioni, M. V. Tratnik, J. E. Sipe, G. L. Oppo [1987] Low instability threshold in a laser operating in both states of polarization, *Optics Letters* **12**, 242–244. (Natural generalizations that govern the dynamics of n-level atoms can also be constructed and yield other types of Maxwell-Bloch systems. These systems are endowed with intrinsic SU(n) symmetries.)

C. Sparrow [1982] *The Lorenz Equations: Bifurcations, Chaos, and Strange Attractors*, Applied Mathematical Sciences 41, New York: Springer-Verlag.